DOI: 10.61782/fa.2025.0961

FORUM ACUSTICUM EURONOISE 2025

VISCOELASTIC MODEL: THE MEMORY OF CEMENT

J. Gosalbez[1*] **V.J. Ruiz**[1] **J. Madrigal**[1]
R. Miralle[1] **I. Bosch** [1] **J. Quiroga**[3] **J. Payá**[1]
[1] Inst. de Telecomunicaciones y Aplicaciones Multimedia. Universitat Politècnica de València. Spain
[2] Instituto de Ciencia y Tecnología del Hormigón, Universitat Politècnica de València. Spain
[3] Universidad Industrial de Santander, Colombia

ABSTRACT

The high sensitivity of nonlinear terms in the elastic response of materials to the early appearance of damage has led to the emergence of the so-called NEWS methods (Non-linear Elastic Wave Spectroscopy). These NDE (Non-Destructive Evaluation) methods exploit the increase in the material's nonlinear behaviour as damage increases. In particular, the NIRAS technique (Non-linear Impact Resonance Acoustic Spectroscopy) detects changes in the resonance of a material (frequency, damping factor, etc.) as a function of impact intensity.
In this work, the NIRAS technique has been employed to characterize concrete using different sensing methods (accelerometers and FBG - Fiber Bragg Grating). Additionally, this study presents the conditioning process, along with a viscoelastic model of the Maxwell and Kelvin-Voigt types, to understand the effects of conditioning on the specimens during testing.

Keywords: *nonlinear acoustics, conditioning effect, fiber Bragg grating (FBG), NIRAS technique*

1. INTRODUCTION

Geomaterials—such as rocks, sand, soil, and combinations thereof like concrete—are classified within a specific group known as Non-Linear Mesoscopic Elastic (NME) materials [1]. These materials are characterized by their heterogeneous internal makeup, with a complex non-linear response strongly influenced by various microstructural elements, including micro-cracks, grain contacts, and voids. Compared to traditional atomic elastic materials, this response is significantly more pronounced. Due to these unique properties, the non-linear behavior of NME materials cannot be adequately described by Landau's classical non-linear elasticity theory [2].

One of the most effective methodologies for evaluating damage in concrete and other cementitious materials is the non-destructive technique known as Nonlinear Elastic Wave Spectroscopy (NEWS). This method focuses on analyzing various nonlinear phenomena [3], including the generation of higher-order harmonics, wave cross-modulation, shifts in resonance frequency, and amplitude-dependent attenuation. Despite variations in technique, all NEWS approaches share a common goal: to quantify non-linear material behaviors through dynamic responses.

Concrete degradation has been extensively studied over time, with research highlighting that different deterioration mechanisms alter their dynamic properties in distinct ways [5][6]. Concrete exposed to thermal shock (rapid temperature changes) can suffer significant internal damage due to the differential expansion and contraction of its constituent materials. This abrupt thermal gradient induces high tensile stresses, particularly at the interfaces between aggregates and the cement paste, often leading to microcracking, debonding, and eventual loss of mechanical integrity. Repeated thermal shocks can accelerate degradation, reducing stiffness, strength, and durability over time [7]. Investigations have applied NEWS techniques to evaluate thermal shock effects on concrete across various compositions and number of cycles [8][9] and changes in

**Corresponding author*: jorgocas@dcom.upv.es

acoustic non-linearity under thermal stress [10][11][12][13].

A notable example is the Non-linear Impact Resonance Acoustic Spectroscopy (NIRAS) technique. NIRAS operates by monitoring how the material's resonance frequency varies with different levels of impact force (see Figure 1), providing insights into internal structural changes.

However, the use of NEWS techniques, and NIRAS in particular, also implies that, under certain conditions, the specimen may undergo a conditioning process as a result of material hysteresis. This leads to observable differences in the results between the first time the material is tested (i.e., non-conditioned state) and subsequent repetitions of the test (conditioned state). This phenomenon can be referred to as discrete memory or material conditioning, and it arises from a combination of slow dynamics and fast dynamics. It is worth noting that the material may or may not return to its relaxed or non-conditioned state over time [4].

In this study, the authors focus on two key aspects. First, they aim to demonstrate the conditioning effect that mortar specimens undergo when subjected to the NIRAS technique. To this end, results from the first (not conditioned status) and second tests (conditioned status) are compared. This conditioning becomes more pronounced in damaged specimens, as non-linear phenomena are more evident in these cases. Therefore, the study specifically considers specimens that have been damaged through thermal shock. Moreover, experiments are conducted using both traditional piezoelectric accelerometers and fiber Bragg grating (FBG) sensors, which are embedded into the specimens during the manufacturing process.

Thanks to the integration of embedded FBG sensors during specimen fabrication, the second objective of this work is to investigate the relaxation behavior of the specimens after being tested. The use of FBG technology allows for internal strain monitoring, offering valuable insight into the time-dependent recovery process that occurs as a result of mechanical conditioning.

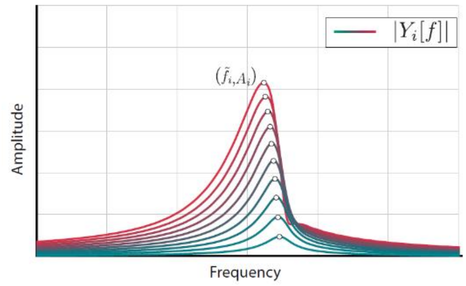

Figure 1. Received frequential response for the different impact levels ($Y_i(f)$)

2. MATHEMATICAL BACKGROUND

NIRAS is a method used for impact assessment and damage detection and involves impacting the material with different strength levels and analyzing the resulting acoustic frequency responses. The different reverberation signals are denoted by $y_i(t)$ where i denotes the different impacts and $Y_i(f)$ is the Fourier Transform of $y_i(t)$ (Figure 1). The non-linear parameters related to the resonance frequency shift α is obtained from a simple linear regression fit (Figure 2):

$$\frac{\tilde{f}_0 - \tilde{f}_i}{\tilde{f}_0} = \alpha \cdot A_i \tag{1}$$

$$A_i = \max|Y_i(f)| \tag{2}$$

$$\tilde{f}_i = \max_f |Y_i(f)| \tag{3}$$

Where A_i is the is the peak amplitude of the spectrum, $\tilde{f}_i$ is the peak frequency and $\tilde{f}_0$ denotes the intersection with y-axis of the linear relationship between the peak amplitudes A_i (x-axis) and the peak frequencies $\tilde{f}_i$ (y-axis).

The NIRAS technique obtains the parameter α_f^{NIRAS}, among others, as an indicator of the no linear behavior of the material: the greater the damage, the greater the no-linear behavior and the greater α_f^{NIRAS}.

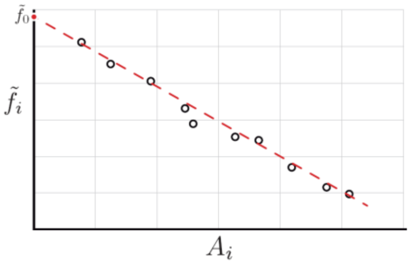

Figure 2. Linear regression from the different resonance signals.

The Maxwell model may be more suitable for describing the dynamic behavior of the specimen during fast mechanical responses, while the Kelvin-Voigt model is more appropriate for representing the slow dynamics effects, such as those associated with conditioning and material relaxation over time. However, experimental observations in this study suggest that both behaviors coexist in the tested specimens. The act of testing itself induces a conditioning state—often referred to as slow dynamics—which subsequently alters the specimen's mechanical response in follow-up impacts, which are governed by fast dynamics.

In this context, the Zener model, derived from a combination or modification of the Maxwell and Voigt models, provides a more comprehensive framework. It effectively captures both the immediate elastic response and the time-dependent relaxation behavior of the tested specimens. Although traditionally used to model fast relaxation phenomena, the results presented in this study and those in [4]demonstrate that damaged specimens, exhibiting stronger non-linear responses, undergo a measurable conditioning process simply as a result of being tested. This effect is clearly reflected in the evolution of the non-linear parameter α reinforcing the connection between mechanical damage, slow dynamics, and non-linear acoustic response.

3. EXPERIMENTAL

3.1 Manufacturing and damage induction of mortar specimens

Three mortar specimens (A, B and C) were prepared by mixing Portland cement (EN 197-1-CEM I 52.5 R) [14], sand (quartz) and water in the 1:3:0.5 ratio. After mixing the components, following the procedure described in UNE-EN 196-1 [15], the fresh mortar was placed in a prismatic mold of 50x60x240 mm size. Because prior to pouring the mortar, several optic fibers were settled according to Figure 4. Due to the fragility of the fibers, the mortar was poured in three layers, avoiding damaging the fibers. For this, the fresh mortar was dropped in a zone free of fiber and then the mold was vibrated (Vibrating Table ToniVIB Tonitechnic) for 30 seconds (vibration frequency 50 Hz, amplitude 1 mm). This procedure was twice repeated and finally the superior part was flattened using a spatula. Additionally, metallic capillary sheath (Figure 3a) was used to protect each optical fiber during the pouring and vibration process and was removed immediately after the surface leveling.

The mold was put in a humid chamber (20 ºC, RH>90%) for 24 hours. After this period, the specimens were carefully demolded and were covered with a plastic film, to avoid water evaporation. The wrapped specimens were stored in the same humid chamber for 46 days, to complete the hydration of the Portland cement.

After 88 days from mixing the mortar components, two of the specimens were subjected to thermal shock (B and C): the specimens were immersed in hot water (80ºC) for 1 hour and then immediately submerged in cold water (4ºC) for 10 minutes, tank of 0.01 m3.

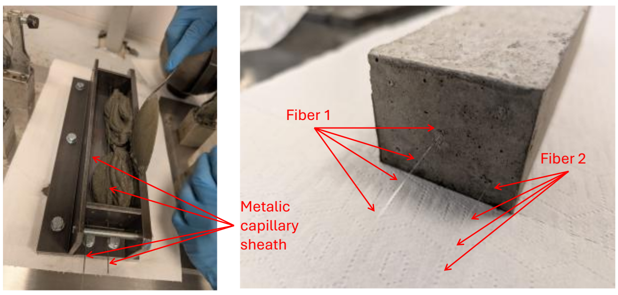

Figure 3. a) Manufacturing process b) Demolded specimen showing the optical fiber emerging from the mortar.

3.2 Embedded Instrumentation

Two of the three specimens (A and B) were internally instrumented during the fabrication process with two optical fibers aligned along the longitudinal axis of the specimen: one positioned at the center and the other near a corner (Figure 4). Each optical fiber contained two integrated Fiber Bragg Gratings (FBGs), which were located at the center and at one end of the fiber.

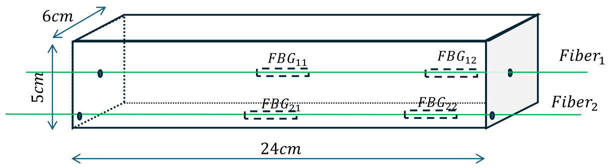

Figure 4. Representación de las fibras embebidas.

The FBGs were primarily tuned to the wavelengths listed in Table 1 and illustrated in Figure 5. Fiber 2 of Mortar A was damaged during the demolding process, therefore no measurements were obtained from this fiber.

Table 1. Wavelengths of the FBGs (nm)

Specimens	$Fiber_1$		$Fiber_2$	
	FBG_{11}	FBG_{12}	FBG_{21}	FBG_{22}
Mortar A	1533.98	1544.05	-	-
Mortar B	1534.07	1543.94	1553.95	1563.80

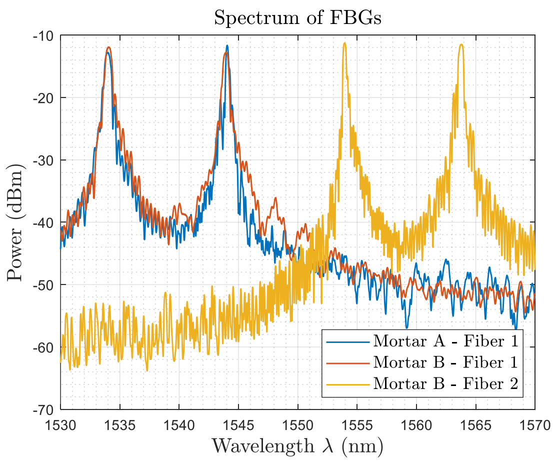

Figure 5. Spectrum of embebed fibers

3.3 Measurement setup

Two distinct experimental configurations were employed in the development of this study. In the first experimental, multiple impacts were applied to different specimens with the objective of analyzing the mechanical conditioning process induced by repeated excitation.

The second setup was designed to perform long-duration measurements, spanning a period of several days. In this case, the specimen was initially subjected to controlled impacts to induce a conditioned state, after which continuous monitoring was carried out with the aim of evaluating the temporal evolution of the material. The main objective was to observe the potential residual effects of the conditioning, as well as the gradual recovery of the specimen's original state once the excitation had ceased.

Both experiments were structured into three functional stages: an initial excitation phase using impact, a second sensing phase, and finally, a data acquisition system responsible for recording and storing the signals obtained.

In the first experiment, the excitation stage consisted of an instrumented hammer and a clamping system designed to immobilize the specimen during measurements, thereby ensuring consistent conditions for each impact. The hammer's attachment to the support allowed for an almost constant impact force across all repetitions, ensuring the repeatability of the conditioning process.

In the second experiment, aimed at studying the temporal evolution of the material, excitation was carried out solely using a conventional hammer, employed to induce the initial conditioning of the specimen prior to the start of prolonged monitoring. In this case, impact uniformity was not critical, as the primary interest lay in observing the post-conditioning effects over time.

During the sensing phase, two types of sensors were used: accelerometers and optical fibers with embedded Fiber Bragg Gratings (FBGs) within the specimens.

In the first experiment, both types of sensors were employed. One accelerometer was placed on the hammer to capture the impact during striking, and another was mounted on the specimen to monitor the material's dynamic response and evaluate the effect of the conditioning induced by repeated impacts. In addition, FBG optical sensors embedded within the specimen were used to record both the impacts and the structural changes in the material resulting from the conditioning process.

In the second experiment, only FBG optical sensors were used, as the main objective was to analyze how the specimen, after being conditioned by the impacts, returned to its initial state or, alternatively, experienced a progressive loss of the properties induced by the conditioning. In this context, the use of accelerometers was not necessary, since the focus was on observing the temporal evolution of the material properties under resting conditions following the initial impacts.

The final stage of the experiment corresponds to data acquisition, for which two specific devices were used, each responsible for capturing data from the different sensors.

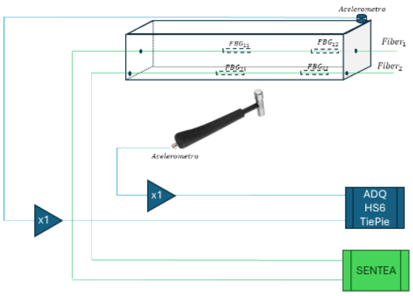

Figure 6. Esquema del montage.

In the first experiment, both devices were used. For the capture of accelerometer data, the TiePie HS6 data acquisition system was employed, which has four input channels. However, in this measurement, only two of these channels were used, dedicating one to each accelerometer (one for the hammer and the other for the specimen).

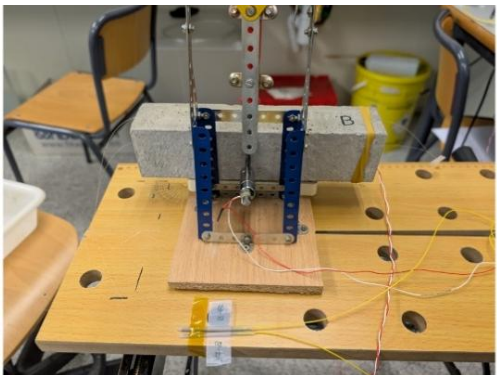

Figure 7. Photograph of the experiment

The second device used was the SENTEA optical interrogator, specifically designed for reading Fiber Bragg Gratings (FBGs). This device also has four channels, allowing for the simultaneous interrogation of multiple FBGs per channel. In the context of this experiment, each channel was used to interrogate a set of FBGs embedded within the specimen, enabling the capture of relevant data on the material's behavior.

In the second experiment, only the SENTEA interrogator was used, as the objective of the measurement focused exclusively on monitoring the FBGs, without the need to record data from the accelerometers.

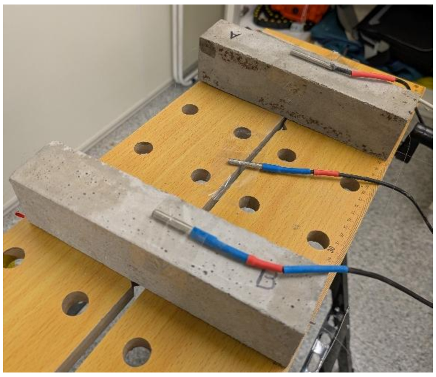

Figure 8. Overview of the long-term experimental setup

In the first experiment, the specimen was placed on a rigid support to prevent any displacement during the measurements (Figure 7). Ten consecutive impacts were applied using the instrumented hammer, with an increasing force in each strike. This process was repeated after the initial ten impacts, allowing for a comparison between measurements obtained under two conditions: one with the specimen in its initial (resting) state, and the other after it had been conditioned by the repeated impacts.

In the second experiment (Figure 8), the specimen was subjected to ten initial impacts in order to induce conditioning. Afterwards, it was left at rest for several days to observe its behavior over time, allowing for the evaluation of whether the specimen gradually returned to its original state or remained in a partially conditioned state. The main objective of this experiment was to analyze the temporal evolution of the material's properties, observing either a return to normality or a progressive loss of the conditioning induced by the impacts.

4. TESTS DESCRIPTION AND RESULTS

As described, two types of tests were conducted on the mortar specimens: the NIRAS acoustic spectroscopy test and the long-term conditioning evolution test. These tests were performed on both undamaged and damaged specimens, using embedded fiber Bragg gratings (FBGs) and piezoelectric accelerometers for strain and vibration measurement. Specifically, three specimens were studied: one undamaged specimen (A) and two thermally shock damaged specimens (B and C). Specimens A and B were instrumented with embedded FBG sensors. The complete experimental matrix is summarized in Table 2.

Table 2. List of damaged and undamaged mortar samples tested with accelerometers and FBGs, non-conditioned (M1) and conditioned (M2) and long-term monitoring

Sample	Status	Acc.		FBG		
		NIRAS				Long-term
		M1	M2	M1	M2	
A	Sound	√	√	√	√	√
	Damage	Reference sample – no damage applied				
B	Sound	√	√	√	√	-
	Damage	√	√	√	√	√
C	Sound	√	√	Not instrumented		
	Damage	√	√			

The first test, the NIRAS procedure, consisted of applying ten controlled impacts to the specimen using an instrumented hammer. The impacts were progressively stronger, modulated by increasing the striking angle. A second identical series of ten impacts was then performed. The first measurement set (M1) corresponds to the non-conditioned state, while the second (M2) corresponds to the conditioned state. This protocol enabled a direct comparison of the specimen's dynamic response before and after conditioning, allowing for the assessment of non-linear and hysteretic behavior resulting from damage. As shown in Figure 9 and Figure 10 the relationship between peak frequency and amplitude, exhibits a consistent variation between the first and second series. While the absolute change may be small, the trend is systematic. Since α is associated with the degree of non-linear behavior, this conditioning effect becomes more evident in the damaged specimens, where non-linearities are more pronounced.

Table 3 and Table 4 summarize the values of both α and f_0 for undamaged and damaged specimens, as well as for the first and second measurement series. For undamaged samples, α is close to zero, indicating an essentially linear material response within the applied impact range (i.e., resonance frequency does not depend on impact amplitude). As damage increases, the absolute value of α also increases, reflecting stronger non-linear behavior. The trend is consistent across both sensing technologies. Additionally, a decrease in f_0 is observed as damage progresses, consistent with a loss of mechanical stiffness. A systematic shift in both α and f_0 is also evident when comparing results from the first impact series (non-conditioned state) with subsequent impacts (conditioned state). This shift is more significant in damaged specimens, which display a more prominent hysteretic response.

Moreover, as shown in Table 3 and Table 4, the parameter α also varies consistently not only between the two damaged specimens but also between the two sensing technologies, reinforcing the robustness of the observed trends.

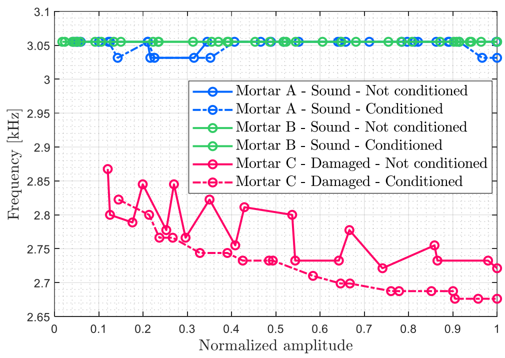

Figure 9. Amplitude vs. frequency curves measured with the accelerometer for conditioned and unconditioned specimens, with and without damage

Table 3. NIRAS parameters (α and f_0) for the samples A, B and C, between "Not conditioned" and "Conditioned" for the accelerometer sensor

		Not conditioned			Conditioned		
Accel.		$-\alpha$	f_0	R^2	$-\alpha$	f_0	R^2
A	Sound	5.77	3.04	0.06	1.14	3.0	0.01
B	Sound	0	3.05	-	0	3.05	-
	Dam.	94	2.78	0.7	106	2.8	0.70
C	Dam.	119	2.8	0.8	148	2.83	0.89

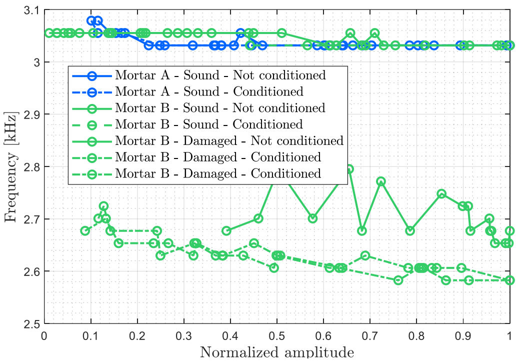

Figure 10. Amplitude vs. frequency curves measured with the FBG for conditioned and unconditioned specimens, with and without damage

Table 4. NIRAS parameters (α and f_0) for the samples A, B and C, between "Not conditioned" and "Conditioned" for one of the FBG sensor

		Not Conditioned			Conditioned		
FBG		$-\alpha$	f_0	R^2	$-\alpha$	f_0	R^2
A	Sound	30.0	3.05	0.37	30.5	3.05	0.38
B	Sound	27	-	0.58	32	3.07	0.77
	Dam.	-	-	-	109	2.68	0.85
C	Dam.	-	-	-	-	-	-

Thanks to the embedded nature of the FBG sensors, it was possible to perform a long-term strain monitoring following the NIRAS impact testing. This second experimental phase involved continuous tracking of the FBG wavelength shift for three days after the initial test. The post-impact wavelength evolution differed significantly between the undamaged and damaged specimens. In the undamaged sample, the wavelength showed a specific temporal trend which correlates with temperature changes, while in the damaged sample, the evolution also followed the temperature changes but with a distinct pattern. This difference can serve as an indicator of two key aspects: the first one the thermal response, since Figure 11 shows that the major wavelength variations coincide with temperature fluctuations; and second one , mechanical relaxation, given that both samples were kept in the same ambient conditions (temperature, humidity, and pressure), allowing the observed trend differences to be attributed to differences of material relaxation dynamics.

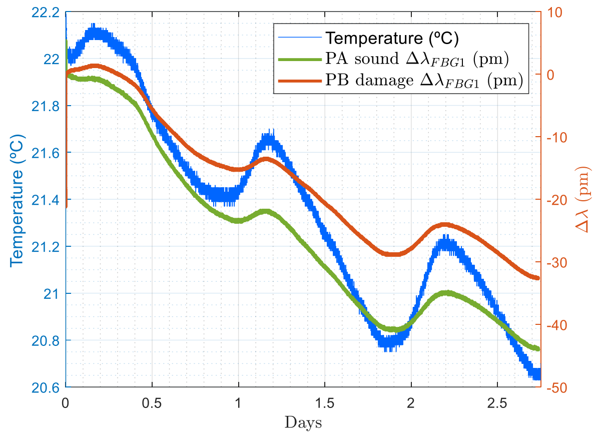

Figure 11. Temperature (blue line), wavelength of sound probe (A) (green line) and wavelength of damaged probe (B) (red line) along several days.

5. CONCLUSIONS

The ability to inspect instrumented specimens, with multiple sensing points along the same fiber, represents a valuable advancement in non-destructive evaluation techniques. The NIRAS technique has proven to be a highly sensitive method for detecting generalized damage. In this study, it was successfully applied to evaluate mortar specimens subjected to thermal shock damage and the comparison between undamaged and damaged samples confirmed the technique's sensitivity.

Furthermore, the study has revealed the presence of a conditioning effect, where specimens exhibit a distinct change in their dynamic response simply as a result of being tested. This was evidenced by systematic differences in the extracted parameters between the first test (non-conditioned state) and subsequent tests (conditioned state). In essence, the material exhibits a form of mechanical memory, which becomes increasingly prominent as damage severity increases.

Two distinct sensing technologies were utilized: traditional piezoelectric accelerometers and embedded fiber Bragg gratings (FBGs). Both demonstrated consistent trends. The accelerometers provided precise results with low variance and high repeatability but required surface attachment. On the other hand, embedded FBGs, despite being more challenging to measure, allowed for similar results while offering the unique capability of long-term internal monitoring.

Thanks to this capability, the FBG sensors enabled the observation of post-test relaxation behavior, highlighting significant differences in the relaxation dynamics between damaged and undamaged specimens. This suggests that FBGs not only replicate conventional measurements but also provide additional insight into the temporal evolution of mechanical conditioning.

6. ACKNOWLEDGMENTS

Grant PID2020-120262GB-I00 funded by MCIN/AEI/ 10.13039/501100011033
2

7. REFERENCES

[1] R. A. Guyer, P. A. Johnson, Nonlinear Mesoscopic Elasticity: Evidence for a New Class of Materials, *Physics Today* 52 (4), 30, 1999.

[2] L. D. Landau, E. M. Lifshitz, "Theory of Elasticity, Pergamon", Oxford, England, 3rd edn., 1986.

[3] L. Ostrovsky, P. A. Johnson, "Dynamic nonlinear elasticity in geomaterials", *Rivista del Nuovo Cimento 24,* 1–46, 2001

[4] A. Carrión, V. Genovés, G. Pérez, J. Bittner, J.S. Popovics, J. Payá, J. Gosálbez, Effects of slow dynamics and conditioning on non-linear hysteretic material assessment using impact resonance acoustic spectroscopy, Mechanical Systems and Signal Processing, 150 (2021)

[5] P. C. Aïtcin, "Binders for durable and sustainable concrete", *CRC Press*, 2014.

[6] M. Alexander, S. Mindess, "Aggregates in concrete", *CRC Press*, 2010.

[7] Neville, A. M., "Properties of Concrete" (5th ed.). *Pearson Education*, 2011

[8] Eiras, J. N., et al., "Nonlinear Ultrasonic Evaluation of Thermal Damage in Concrete." Cement and Concrete Research, 80, 31–39, 2016

[9] Payan, C., Garnier, V., Moysan, J., & Johnson, P. A.. "Applying Nonlinear Resonant Ultrasound Spectroscopy to Improve Thermal Damage Assessment in Concrete." *Journal of the Acoustical Society of America*, 121(4), EL125–EL130, 2007

[10] C. Payan, et. al., "Probing material nonlinearity at various depths by time reversal mirrors", *Applied Physics Letters* 104 (14), 144102, 2014.

[11] C. Payan, T. J. Ulrich, P.-Y. Le Bas, T. Saleh, M. Guimaraes, "Quantitative linear and nonlinear resonance inspection techniques and analysis for material characterization: Application to concrete thermal damage", *The Journal of the Acoustical Society of America* 136 (2), 537–546, 2014.

[12] H. J. Yim, J. H. Kim, S.-J. Park, H.-G. Kwak, "Characterization of thermally damaged concrete using a nonlinear ultrasonic method", *Cement and Concrete Research* 42 (11), 1438–1446, 2012.

[13] Chen, J., Bharata, R., Yin, T. et al. "Assessment of sulfate attack and freeze–thaw cycle damage of cement-based materials by a nonlinear acoustic technique". *Mater Struct* 50, 105, 2017.

[14] AENOR, "UNE-EN 197-1. Cement. Part 1: Composition, specifications and conformity criteria for common cements.," 2011. [Online]. Available: www.aenor.es

[15] AENOR, "UNE-EN 196-1. Methods of testing cement. Part 1: Determination of strength.," 2018.